

Article

# Increased Temperature and Nitrogen Enrichment Inhibit the Growth of the Golden Tide Blooming Macroalgae *Sargassum horneri* in the Yellow Sea, China

Hailong Wu<sup>1,2</sup>, Xuebing Li<sup>1,2</sup>, Yanhong Liu<sup>1,2</sup>, Chuchu Wang<sup>1,2</sup>, Chenkai Ji<sup>1,2</sup> and Juntian Xu<sup>1,2,\*</sup>

<sup>1</sup> Jiangsu Key Laboratory of Marine Bioresources and Environment, Jiangsu Ocean University, Lianyungang 222005, China

<sup>2</sup> Co-Innovation Center of Jiangsu Marine Bio-Industry Technology, Jiangsu Ocean University, Lianyungang 222005, China

\* Correspondence: jtxu@jou.edu.cn; Tel./Fax: +86-(0)-518-8558-5003

**Abstract:** The golden tide, a large biomass bloom of the brown macroalgae *Sargassum horneri*, occurs yearly in the Yellow Sea, where it causes enormous economic and ecologic losses. To investigate the response of *S. horneri* to global warming and eutrophication, *S. horneri* was cultured under six conditions of varying temperature combinations (20 and 24 °C) and nitrogen levels (5, 30, and 300 µM). The growth, photosynthetic performance, pigment content, and contents of soluble protein were assessed. The growth of *S. horneri* followed an increasing trend with increasing N concentration at ambient temperature. Elevated temperatures had an inhibitory effect on growth and photosynthesis in *S. horneri*, which was further enhanced by eutrophication. This suggests that in the globally warming environment of the future, eutrophication may reduce the frequency and scale of gold tide outbreaks during the hot season.

**Keywords:** blooming mechanisms; golden tide; elevated temperature; nitrogen enrichment; *Sargassum horneri*



**Citation:** Wu, H.; Li, X.; Liu, Y.; Wang, C.; Ji, C.; Xu, J. Increased Temperature and Nitrogen Enrichment Inhibit the Growth of the Golden Tide Blooming Macroalgae *Sargassum horneri* in the Yellow Sea, China. *J. Mar. Sci. Eng.* **2022**, *10*, 1692. <https://doi.org/10.3390/jmse10111692>

Academic Editor: Valerio Zupo

Received: 21 September 2022

Accepted: 3 November 2022

Published: 8 November 2022

**Publisher's Note:** MDPI stays neutral with regard to jurisdictional claims in published maps and institutional affiliations.



**Copyright:** © 2022 by the authors. Licensee MDPI, Basel, Switzerland. This article is an open access article distributed under the terms and conditions of the Creative Commons Attribution (CC BY) license (<https://creativecommons.org/licenses/by/4.0/>).

## 1. Introduction

Since the industrial revolution, the concentration of carbon dioxide (CO<sub>2</sub>) in the atmosphere has continually increased as a result of the massive combustion of fossil fuels and other human activities. This increase in atmospheric CO<sub>2</sub> concentrations will not only increase the acidity of the oceans [1], but will also lead to global warming and higher sea temperatures [2–4]. It has been predicted that the atmospheric CO<sub>2</sub> concentration will reach about 1000 µatm in the atmosphere by the end of the 21st century [5]. In response, sea surface temperatures will rise by 1–3 °C [6]. Variations in the sea surface temperatures have been shown to significantly impact marine life and ultimately also the composition of marine communities [7,8]. Macroalgae are a vital element of the primary productivity of marine ecosystems, because of their high photosynthetic productivity [9]. Recently, a growing number of researchers suggested that macroalgae play an important role in marine carbon sequestration, thus highlighting their importance as a potential measure to mitigate the effects of man-made CO<sub>2</sub> emissions [10–13]. Macroalgae are commonly subject to temperature fluctuations caused by tide, daytime, and seasonal variations in their natural seawater habitat [14,15]. The response of algae to temperature changes is specific. It has been shown that an increase in temperature promotes the growth of the brown macroalga *Sargassum horneri* [16]. However, increasing temperatures may have negative effects on phytoplankton productivity, biomass, and species diversity [17,18]. Earth system models predict that oceanic warming will cause a reduction in ocean phytoplankton primary production by 20% throughout the 21st century [19,20]. To truly and comprehensively identify the response of algae to continuous global warming, a number

of scholars proposed that the physiological properties of algae should be considered at various temperatures [21,22]. Although the interaction between temperature and nutrients on algal growth has been studied [23]. The survival, growth, reproduction, metabolic rate, biochemical composition, and geographical distribution of macroalgae are all significantly affected by temperature [24]. In aquatic ecosystems, temperature and nutrient availability are the main drivers of phytoplankton productivity [25]. Under the context of global warming, coastal eutrophication caused by human activities cannot be ignored. With the rapid development of mariculture in recent years, the contents of nitrogen (N) and phosphorus (P) in the coastal ecosystem have increased [26]. Eutrophication has been shown to be caused by the excessive availability of organic nutrients, which is one of the major threats to biodiversity and ecosystem functions in the global oceanic environment [27]. Macroalgae can absorb large quantities of N, P, and other nutrients from the seawater, and therefore, play an important role in the alleviation of eutrophication [28,29]. The concentration of nutrients in seawater is a key factor affecting the growth of macroalgae [30,31]. N has been demonstrated to be the most important nutrient for the growth of *Ulva prolifera* because of its higher uptake rate per unit biomass of N compared with P [32–34]. One of the more apparent consequences of eutrophication is that it can lead to algal blooms, such as green tides and golden tides [35]. *S. horneri* is one of the most common macroalgae in China [36]. Because of its huge biomass [37] and strong nutrient absorption capacity, this macroalgae has become the main choice for the reconstruction of algal beds [38]. Since 2010, the gold boom caused by *S. horneri* has received increasing attention [39]. The effect of various nutrients on the physiological properties of *Sargassum* species has been intensively studied [40–42]. It has been shown that nutrient enrichment promotes the growth and photosynthesis of *Sargassum* [40]. However, it has been shown that golden tides caused by *Sargassum natans* were more likely caused by particular oceanographic processes than by eutrophication [35].

Global warming and eutrophication are not isolated events; rather, they are interconnected and occur simultaneously, especially in coastal waters. Temperature and nutrition are the two most powerful drivers of biological processes, thus limiting primary production worldwide [43–45]. The interaction effect of both factors may be completely different or exceed the effect of any single factor. For example, significant differences in temperature and nutrition efficiency were found between phytoplankton species [46,47]. Most previous studies focused on temperature changes below the optimum temperature of the investigated species, and little is known about the interaction between temperature increases beyond the optimum temperature and eutrophication in *S. horneri*. This study selected *S. horneri* and investigated their response to interactions between oceanic warming and eutrophication. The results help to predict the future trends of the occurrence of golden tides caused by eutrophication under the background of global warming.

## 2. Materials and Methods

### 2.1. Sample Collection

In September 2019, *S. horneri* was collected from Weihai (122.12° E, 37.52° N), Shandong Province, China. The dissolved total nitrogen concentration was about  $30 \pm 1.42 \mu\text{mol}\cdot\text{L}^{-1}$ , while the concentration of  $\text{PO}_4\text{-P}$  was  $3.34 \pm 0.21 \mu\text{mol}\cdot\text{L}^{-1}$ . Water samples were analyzed based on the specifications for an oceanographic survey (GB/T 12763.4-2007). The collected macroalga was saved in a cold box and immediately transported to the laboratory. The macroalga was cleaned with sterile seawater by gently rinsing thalli to remove debris and epiphytes. Prior to experiments, healthy *S. horneri* thalli were cultured in bottles containing sterile artificial seawater, enriched with  $30 \mu\text{M NaNO}_3$  and  $10 \mu\text{M KH}_2\text{PO}_4$ . This artificial seawater was continuously aerated and the medium was changed every two days. The temperature was set to  $20 \text{ }^\circ\text{C}$ , the light intensity was set to  $80 \mu\text{mol photons m}^{-2}\text{s}^{-1}$ , and the photocycle was 12:12 h (light: dark). These cultural conditions were controlled by an incubator (Jiangnan, Ningbo, China). After one week of laboratory acclimatization, healthy thalli were randomly selected and used as experimental materials.

## 2.2. Experimental Design

Since the water temperature at the sampling site was about 20 °C, and the expected future temperature under global warming will rise to 4 °C in 2100 (IPCC, 2014) [48], two temperature levels (20 °C, ambient temperature (CT), and 24 °C, elevated temperature (ET)) and other cultural conditions (light intensity: 80  $\mu\text{mol photons m}^{-2}\text{s}^{-1}$ ; photoperiod: 12:12 h (light: dark)) were maintained by two GXZ-300C intelligent light incubators (Jiangnan, Ningbo, China). Three different N concentrations were obtained by controlling the amount of added  $\text{NaNO}_3$ : High N (HN, 300  $\mu\text{M}$ ); intermediate N (IN, 30  $\mu\text{M}$ ) (simulating ambient nutrient level), and low N (LN, 5  $\mu\text{M}$ ). The following six treatments were investigated: CT + LN, CT + IN, CT + HN, ET + LN, ET + IN, and ET + HN. Each treatment was conducted in three replicates, with a total of 18 bottles in this experiment. Healthy thalli were cultured in round 500-mL bottles containing artificial seawater enriched with 10  $\mu\text{M PO}_4^{3-}$  (to avoid P restriction) and with three N concentrations, at a stocking density of 0.4 g/L. The medium was aerated and replaced every two days. The fresh weight of the macroalgae was measured to assess the algal growth rate. After one week, the chlorophyll fluorescence, photosynthetic rate, pigments, and soluble proteins were measured.

## 2.3. Measurement of Growth

The relative growth rate (RGR) is an important indication of algal growth, measured as the fresh weight of algae. The following equation was used to calculate the RGR:  $\text{RGR} (\% \text{ day}^{-1}) = 100 \times (\ln N_t - \ln N_0) / t$ , where  $N_0$  represents the initial fresh weight,  $N_t$  represents the final fresh weight, and  $t$  represents the number of culture days during the experiment.

## 2.4. Chlorophyll Fluorescence Measurements

The relative electron transfer rate (rETR), the effective quantum yield ( $F_v'/F_m'$ ), and the maximum quantum yield ( $F_v/F_m$ ) of *S. horneri* were measured using the Aqua Pen fluorometer (AP-C 100, PSI, Berlin, Germany). The  $F_v/F_m$  of *S. horneri* was obtained after a saturation pulse (5000  $\mu\text{mol photons m}^{-2}\text{s}^{-1}$ , for 0.6 s), after 15 min of dark acclimatization. The rETR was calculated as follows [49]:

$$\text{rETR} (\mu\text{mol e}^- \text{ m}^{-2} \text{ s}^{-1}) = \text{yield} \times 0.5 \times \text{PAR}, \quad (1)$$

where yield represents the effective photosynthetic quantum yield of PSII, 0.5 is the ratio of absorbed light to total incident light, and PAR represents the actual light intensity ( $\mu\text{mol photons m}^{-2}\text{s}^{-1}$ ). The rapid light curves were determined under different photosynthetically active photon fluxes. The fitting formula is shown in the following [50]:

$$\text{rETR} = P_m \times \tanh(\alpha \times \text{PAR}/P_m) \quad (2)$$

## 2.5. Measuring the Photosynthetic Rate

The photosynthetic oxygen evolution of *S. horneri* was measured using a Clark-type oxygen electrode (YSI model 5300A, Yellow Springs, OH, USA). The temperature was constantly controlled at either 20 °C or 24 °C by an LKB constant temperature water circulator (DHX-2005, Xianou, Nanjing, China), separately. The macroalgae *S. horneri* thalli were cut into segments of 1 cm length, and then restored under growth conditions for 1 h. Approximately 0.02 g of *S. horneri* (fresh weight) was transferred to an oxygen electrode chamber containing 8 mL of artificial medium to determine photosynthesis. Decreased values of oxygen content in seawater were defined as the respiration rate after 5 min of acclimatization to darkness, while increased values were defined as the net photosynthetic rates in response to the cultivation light density (80  $\mu\text{mol photons m}^{-2}\text{s}^{-1}$ ), respectively.

## 2.6. Pigments Measurement

About 0.02 g of *S. horneri* (fresh weight) was dissolved in 10 mL of absolute methanol at 4 °C for 24 h in darkness [51]. The contents of photosynthetic pigments (chlorophyll- $\alpha$  (Chl *a*) and carotenoids (Car)) were estimated according to Wellburn (1994) [52].

### 2.7. Soluble Protein Determination

Soluble protein (SP) contents in *S. horneri* were determined via Coomassie Brilliant Blue G-250 dye combination according to Kochert (1978) [53]. Approximately 0.02 g of *S. horneri* (fresh weight) was homogenized in a mortar with phosphoric acid buffer. The solution was diluted to 10 mL with buffer, centrifuged at 5000 rpm for 15 min, and then used to determine the SP content using an ultraviolet spectrophotometer. The absorbance of the supernatant was recorded at 595 nm. Bovine serum albumin (BSA) was used as the standard.

### 2.8. Data Analysis

The results were expressed as means of replicates  $\pm$  standard deviations. Data were processed by Origin 2018 software, using one-way analysis of variance (ANOVA) (Tukey's post hoc test) or multiple comparisons to analyze the difference between treatments. Two-way ANOVA was conducted to assess the interactive effects of temperature and N concentration.  $p < 0.05$  was considered to represent a significant difference, which was indicated by different letters in figures.

## 3. Results

The influence of temperature and N concentration on the growth of *S. horneri* is shown in Figure 1. Two-way ANOVA analysis indicated that both temperature and N concentration had an interactive effect, and temperature exerted a major effect on the RGR of *S. horneri* (see Table 1). A posthoc Tukey HSD comparison showed that there was no significant difference in the RGR of *S. horneri* under elevated temperature regardless of N concentration ( $p > 0.05$ ). The RGR of *S. horneri* followed a slowly declining trend with increasing N concentration. Then, at normal temperature, the RGR of *S. horneri* followed an increasing trend with increasing N concentration, and the RGR of the high N condition was significantly higher than those of both low N and intermediate N ( $p < 0.05$ ). In addition, at the same N concentration, the elevated temperature decreased the RGR of *S. horneri*. At elevated temperatures, the RGR was significantly lower than at normal temperatures ( $p < 0.05$ ).

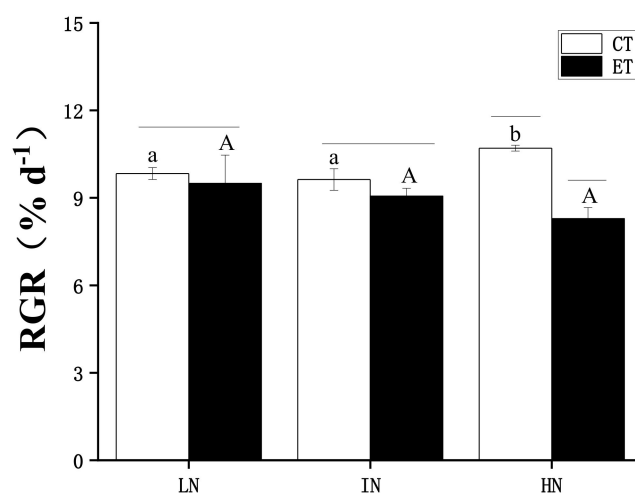


**Figure 1.** Relative growth rate (RGR) of *Sargassum horneri* under low nitrogen (LN), intermediate N (IN), and high N (HN) treated by ambient temperature (CT) and elevated temperature (ET) during the experiment. Data are means  $\pm$  SD ( $n = 3$ ). Horizontal lines represent significant differences ( $p < 0.05$ ) among the temperature levels at the same N concentration, the different capital letters represent significant differences ( $p < 0.05$ ) among N concentrations at the elevated temperature, while the different lower-case letters represent significant differences ( $p < 0.05$ ) among N concentrations at the ambient temperature.

**Table 1.** Two-way analysis of variance (ANOVA) for the effects of different temperatures and nitrogen (N) concentrations on the relative growth rate (RGR) of *Sargassum horneri*. Abbreviations: degree of freedom (DF), value of the F statistic (F-value).

Source	RGR (% d <sup>-1</sup> )		
	DF	F-Value	p-Value
Temperature	1	24.68844	<0.001
N concentration	2	0.69394	0.51858
Temperature*N concentration	2	8.72092	0.00458

The  $Fv'/Fm'$  and  $Fv/Fm$  of *S. horneri* at different N concentrations and temperatures are shown in Figure 2. Two-way ANOVA analysis indicated that both temperature and N concentration had an interaction effect, where temperature played a major role (Table 2). A posthoc Tukey HSD comparison showed that, under the same temperature conditions, regardless of N concentration, the  $Fv'/Fm'$  of *S. horneri* was not significantly different ( $p > 0.05$ ). At the low N and intermediate N conditions, the elevated temperature only increased  $Fv'/Fm'$  under the condition of high N ( $p < 0.05$ ).  $Fv/Fm$  showed a similar response trend to  $Fv'/Fm'$ , where elevated temperature played a significant role. Under the conditions of intermediate N and high N, elevated temperature significantly promoted  $Fv/Fm$  ( $p < 0.05$ ). At ambient temperature,  $Fv/Fm$  was significantly higher for low N than for intermediate N and high N ( $p < 0.05$ ), while other differences were not significant ( $p > 0.05$ ).

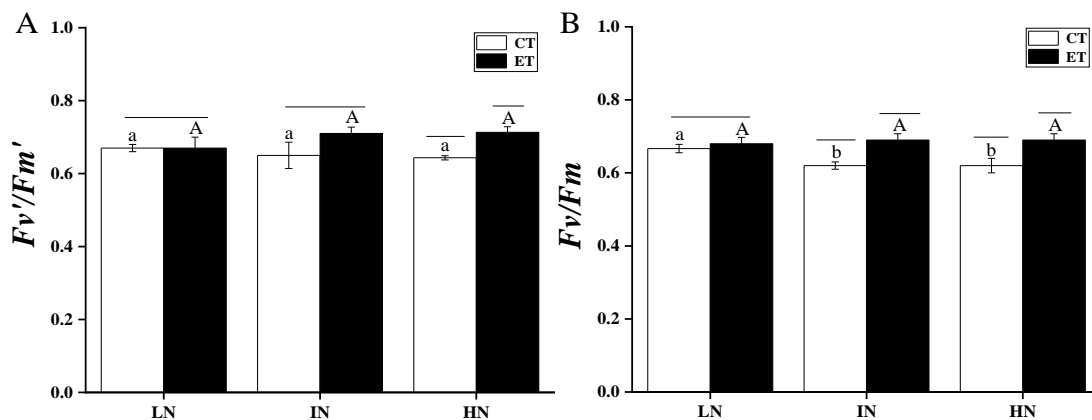


**Figure 2.** The effective quantum yield ( $Fv'/Fm'$ ) (A) and maximum quantum yield ( $Fv/Fm$ ) (B) of *S. horneri* under LN, IN, and HN treated by CT and ET. Data are means  $\pm$  SD ( $n = 3$ ). Horizontal lines represent the significant difference ( $p < 0.05$ ) among the temperature levels at the same N concentration, the different capital letters represent significant differences ( $p < 0.05$ ) among N concentrations at the elevated temperature, while the different lower-case letters represent significant differences ( $p < 0.05$ ) among N concentrations at the ambient temperature.

**Table 2.** Results of two-way ANOVA for *S. horneri* under low nitrogen (LN), intermediate N (IN), and high N (HN) treated by ambient temperature (CT) and elevated temperature (ET).

Source	DF	F-Value	p-Value
<i>Fv'/Fm'</i>			
Temperature	1	17.68605	0.00122
N concentration	2	0.36047	0.70465
Temperature*N concentration	2	4.5	0.03482
<i>Fv/Fm</i>			
Temperature	1	46	<0.001
N concentration	2	2.63043	0.1129
Temperature*N concentration	2	6.28261	0.01359

The effects of temperature and N concentration on the chlorophyll fluorescence parameters of *S. horneri* are shown in Figure 3 and Table 3. Two-way ANOVA analysis identified an interaction between temperature and N concentration, which affected the maximum relative electron transfer rate ( $rETR_{max}$ ), light energy utilization rate ( $\alpha$ ), and saturated light intensity ( $I_k$ ). Temperature strongly affected the chlorophyll fluorescence parameters of *S. horneri* (Table 4). At normal temperatures, high N significantly inhibited  $rETR_{max}$ ,  $\alpha$ , and  $I_k$  ( $p < 0.05$ ), while elevated temperature alleviated this inhibition. At the same N concentration, an increase in temperature promoted  $rETR_{max}$ ,  $\alpha$ , and  $I_k$ , while increased N concentration aggravated this promotion ( $p < 0.05$ ). In addition, at elevated temperatures,  $I_k$  was only significantly lower in the low N condition compared with the intermediate N condition and the high N condition ( $p < 0.05$ ). The influences of other N concentrations on  $rETR_{max}$ ,  $\alpha$ , and  $I_k$  were not significant ( $p > 0.05$ ).

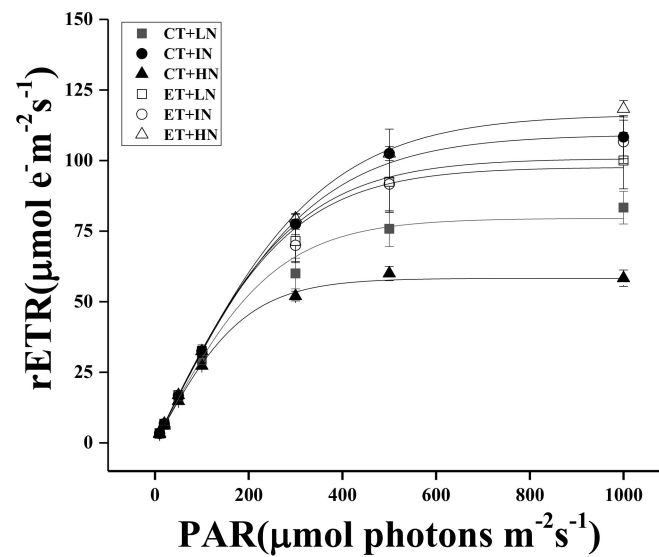


**Figure 3.** Rapid light curve (RLC) of photosynthetic system II (PSII) of *S. horneri* under LN, IN, and HN, treated by CT and ET. Data are means  $\pm$  SD ( $n = 3$ ).

**Table 3.** Photosynthetic parameters of the rapid light curve of *S. horneri* under LN, IN, and HN treated by CT and ET.  $rETR_{max}$  represents the maximum relative electron rate,  $\alpha$  represents the light harvesting efficiency, and  $I_k$  represents the photosynthesis saturated light intensity. Significant differences are indicated by different letters (one-way ANOVA), and values represent the mean  $\pm$  SD ( $n = 3$ ). \* represents a significant difference ( $p < 0.05$ ) among temperature levels at the same N concentration, the different capital letters represent significant differences ( $p < 0.05$ ) among N concentrations at the elevated temperature, while the different lower-case letters represent significant differences ( $p < 0.05$ ) among N concentrations at the ambient temperature.

Treatments	$rETR_{max}$ $\mu\text{mol e}^- \text{m}^{-2} \text{s}^{-1}$	$\alpha$	$I_k$ $\mu\text{mol Photos m}^{-2} \text{s}^{-1}$
CT + LN	$82.19 \pm 6.17^a$	$0.27 \pm 0.02^a$	$299.58 \pm 17.14^a$
CT + IN	$110.17 \pm 8.64^b$	$0.33 \pm 0.01^b$	$331.61 \pm 13.53^{a*}$
CT + HN	$59.14 \pm 2.49^{c*}$	$0.29 \pm 0.01^{b*}$	$202.46 \pm 9.30^{b*}$
ET + LN	$100.28 \pm 11.11^A$	$0.31 \pm 0.03^A$	$318.82 \pm 24.23^A$
ET + IN	$106.03 \pm 8.76^A$	$0.29 \pm 0.02^A$	$362.15 \pm 12.89^{B*}$
ET + HN	$118.59 \pm 2.96^{A*}$	$0.32 \pm 0.01^{A*}$	$368.80 \pm 3.42^{B*}$

**Table 4.** Results of two-way ANOVA for photosynthetic parameters derived from the rapid light curves (RLCs) of PSII of *S. horneri* under LN, IN, and HN, treated by CT and ET.

Source	DF	F-Value	p-Value
rETR <sub>max</sub>			
Temperature	1	49.34006	<0.001
N concentration	2	12.08173	0.00133
Temperature*N concentration	2	28.61007	<0.001
α			
Temperature	1	1.11486	0.31182
N concentration	2	1.18812	0.33823
Temperature*N concentration	2	6.75108	0.01085
Ik			
Temperature	1	105.50349	<0.001
N concentration	2	25.87745	<0.001
Temperature*N concentration	2	45.41122	<0.001

The effects of temperature and N concentration on the net photosynthetic rate and the dark respiration rate of *S. horneri* are shown in Figure 4. Two-way ANOVA analysis indicated that both temperature and N concentration had an interaction effect, which affected both the net photosynthetic rate and the dark respiration rate of *S. horneri* (Table 5). The effect of N concentration was not significant at ambient temperature ( $p > 0.05$ ). Increasing the temperature significantly promoted the net photosynthetic rates ( $p < 0.05$ ), while this effect could be offset by increasing the N concentration. The difference in the net photosynthetic rate of the two temperatures was not significant ( $p > 0.05$ ) under the high N condition only. With regard to the dark respiration rate, the impact of increasing temperature at low N was not significant ( $p > 0.05$ ). At intermediate N concentration, elevated temperature significantly inhibited the dark respiration rate ( $p < 0.05$ ), while elevated temperature significantly increased the dark respiration rate at high N ( $p < 0.05$ ). The dark respiration rate under intermediate N was significantly higher than that of low N and high N under normal temperature ( $p < 0.05$ ). The dark respiration rate at high N was significantly higher than at both low N and intermediate N under elevated temperature ( $p < 0.05$ ).

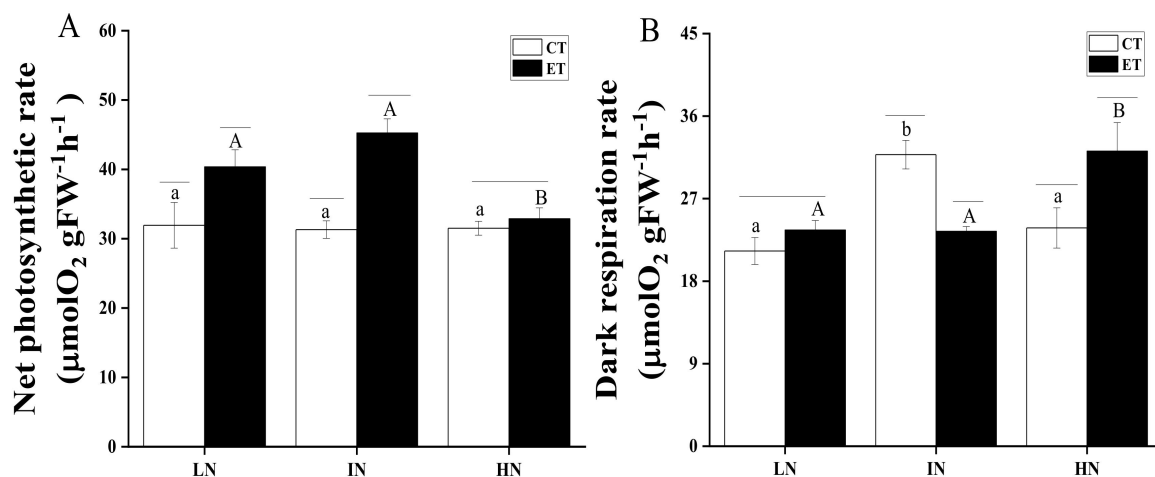


**Figure 4.** Net photosynthetic rate(A) and dark respiration rate (B) of *S. horneri* under LN, IN, and HN, treated by CT and ET. Data are means  $\pm$  SD (n = 3) Horizontal lines represent significant differences ( $p < 0.05$ ) among the temperature levels at the same N concentration, the different capital letters represent significant differences ( $p < 0.05$ ) among N concentrations at the elevated temperature, while the different lower-case letters represent significant differences ( $p < 0.05$ ) among N concentrations at the ambient temperature.

**Table 5.** Results of two-way ANOVA for net photosynthetic rate (NPR) and dark respiration rate (DRR) of *S. horneri* under LN, IN, and HN, treated by CT and ET.

Source	DF	F-Value	p-Value
NPR			
Temperature	1	64.89353	<0.001
N concentration	2	13.19405	<0.001
Temperature*N concentration	2	13.71753	<0.001
DRR			
Temperature	1	0.79293	<0.001
N concentration	2	17.09959	<0.001
Temperature*N concentration	2	31.733	<0.001

The effects of temperature and N concentration on the photosynthetic pigments of *S. horneri* are shown in Figure 5. Two-way ANOVA analysis indicated that both temperature and N concentration had an interaction effect, which affected the photosynthetic pigments of *S. horneri* (Table 6). Chl *a* and Car followed the same trend. Under low N and intermediate N, Chl *a* and Car did not change significantly by increasing the temperature ( $p > 0.05$ ), while elevated temperature significantly increased the contents of Chl *a* under high N ( $p < 0.05$ ). In the conditions with elevated temperatures, the amount of Chl *a* under the high N concentration was significantly higher than under both low N and intermediate N concentrations ( $p < 0.05$ ). Under ambient temperature conditions, the amount of Car in high N was significantly lower than that of low N and intermediate N ( $p < 0.05$ ).

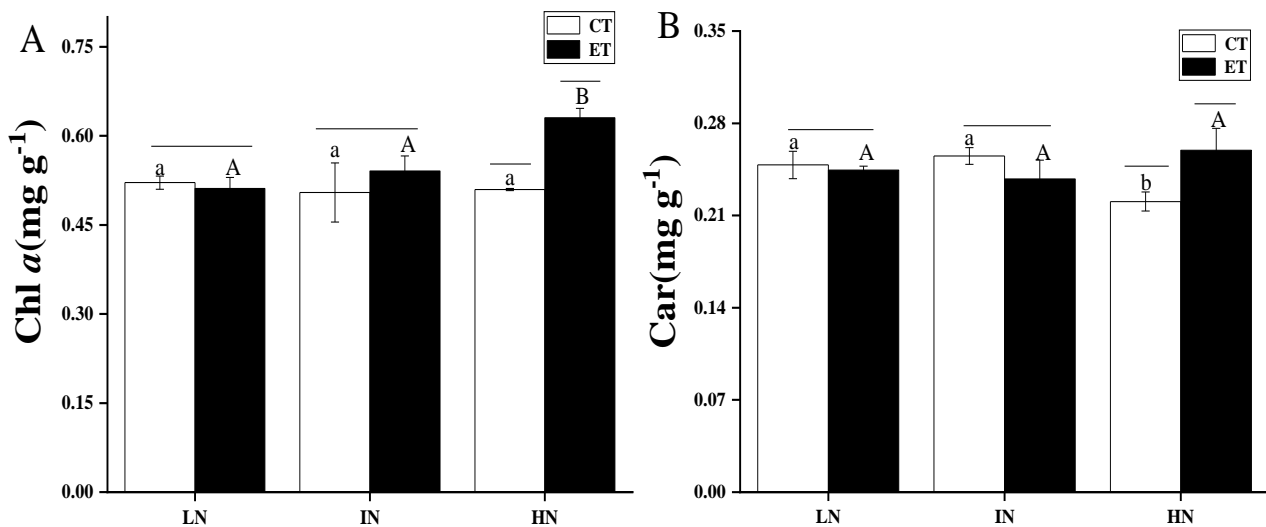


**Figure 5.** Contents of Chlorophyll-a (Chl *a*) (A) and carotenoids (Car) (B) of *S. horneri* under LN, IN, and HN treated by CT and ET. Data are means  $\pm$  SD (n = 3). Horizontal lines represent the significant difference ( $p < 0.05$ ) among the temperature levels at the same N concentration, the different capital letters represent significant differences ( $p < 0.05$ ) among N concentrations at the elevated temperature, while the different lower-case letters represent significant differences ( $p < 0.05$ ) among N concentrations at the ambient temperature.

**Table 6.** Results of two-way ANOVA for chlorophyll  $\alpha$  (Chl  $\alpha$ ) and carotenoids (Car) of *S. horneri* under LN, IN, and HN, treated by CT and ET.

Source	DF	F-Value	p-Value
Chl $\alpha$			
Temperature	1	17.01619	0.00141
N concentration	2	8.08644	0.00597
Temperature*N concentration	2	10.29292	0.00249
Car			
Temperature	1	1.33014	0.27124
N concentration	2	0.71039	0.511
Temperature*N concentration	2	11.3529	0.00171

The effects of temperature and N concentration on the contents of soluble protein in *S. horneri* are shown in Figure 6. Two-way ANOVA analysis ( $p = 0.05$ ) indicated that both temperature and N concentration had an interaction effect, which affected the soluble protein content of *S. horneri* (Table 7). The soluble protein followed the opposite trend than RGR. With increasing N concentration and under ambient temperature, the contents of the *S. horneri* soluble proteins decreased and were significantly lower under high N than under low N ( $p < 0.05$ ). The soluble protein contents decreased in response to elevated temperatures. For all N concentrations, elevated temperature significantly inhibited the content of soluble protein ( $p < 0.05$ ), while an increase in N concentration alleviated this inhibitory effect.

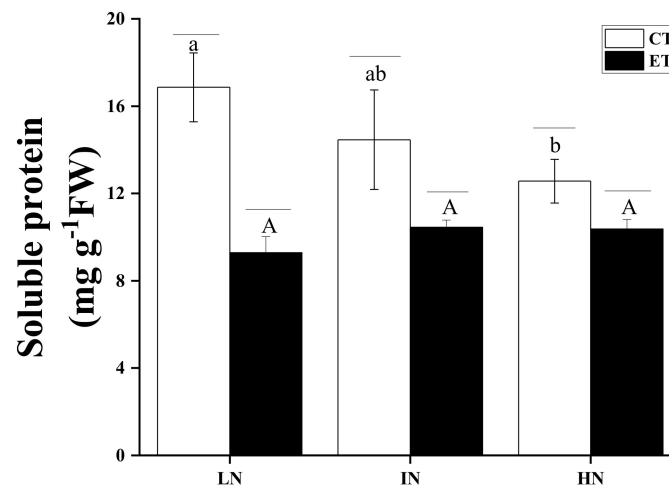


**Figure 6.** Contents of soluble protein (SP) of *S. horneri* under LN, IN, and HN treated by CT and ET. Data are means  $\pm$  SD ( $n = 3$ ). Horizontal lines represent significant differences ( $p < 0.05$ ) among the temperature levels at the same N concentration, the different capital letters represent significant differences ( $p < 0.05$ ) among N concentrations at the elevated temperature, while the different lower-case letters represent significant differences ( $p < 0.05$ ) among N concentrations at the ambient temperature.

**Table 7.** Results of two-way ANOVA for soluble protein (SP) of *S. horneri* under LN, IN, and HN, treated by CT and ET.

Source	DF	F-Value	p-Value
SP			
Temperature	1	59.90949	<0.001
N concentration	2	2.49521	0.12413
Temperature*N concentration	2	7.11245	0.00918

#### 4. Discussion

Global warming caused by increasing CO<sub>2</sub> levels (as a result of the greenhouse effect) challenges the environmental resilience of coastal marine organisms. Macroalgae play a vital role in the processes of the marine ecosystem, particularly in the intertidal zone [9]. Therefore, intertidal macroalgae are often selected as model systems to study the impact of the environment on intertidal organisms [54,55]. Bloom-forming species have been found to be most sensitive to environmental changes. Therefore, blooming species of macroalgae such as *Ulva prolifera* and *Ulva linza* have increasingly attracted attention [16,56,57]. Outbreaks of macroalgal blooms are often associated with eutrophication, which increases their intensity and duration [58].

Growth is a comprehensive expression of various physiological characteristics of algae. When the sea surface temperature was about 20 °C in Weihai, the largest scale of *S. horneri* was observed. The phenomenon is consistent with the previous research which suggested that the optimal growth temperature of adult *S. horneri* was 20 °C [59,60]. Compared with adult blades of *S. horneri*, the optimal growth temperature of seedlings was higher, which was between 20 and 25 °C [60]. The growth would be inhibited under supra- or sub-optimum conditions. In our study, warming induced an inhibitory effect on the growth of *S. horneri*, which was intensified by eutrophication. This differs from the results that both the growth and metabolic rate of macroalgae are promoted by elevated temperatures [61]. This difference likely emerges because the temperatures applied by these other studies remained below the optimal temperature, while the present study uses a temperature above the optimal temperature. Previous studies have shown that the metabolic rate of organisms increases exponentially with increasing temperature; however, after reaching the optimal temperature, the metabolic rate decreases exponentially with increasing temperature [30,62,63]. Even with sufficient availability of nutrients, increasing temperatures can cause growth rates to slow or worsen. Studies predicting the ecological impact of expected temperature changes have shown that many species will be adversely affected during this century, particularly in tropical (i.e., higher temperature) regions [18,64–66]. The present study showed that the growth of *S. horneri* followed an increasing trend with increasing N concentration at ambient temperature. However, under the condition of elevated temperature, the growth of *S. horneri* decreased with increasing N concentration, although this trend was not significant. The N concentration in seawater has been suggested to be a limiting factor of algal growth [67]. In this study, *S. horneri* showed no sensitivity to changing N concentrations. To explain this result, it is first necessary to consider that *S. horneri* itself lives in coastal waters, which are greatly affected by human activities, and that *S. horneri* has wide adaptability to N concentration. Secondly, differences exist between different species of algae, and their response to N concentration is also different. For example, it has been shown that an increased N concentration can promote the growth of *Ulva lactuca* [68]. N enrichment did not affect the growth rates of *Sargassum fluitans* or *Sargassum natans* [69]. In the present study, eutrophication was found to intensify the growth-inhibiting effect under increasing temperature, which may be a result of the interaction between temperature and N concentration.

Previous studies have shown that when exposed to environmental stress, algae can regulate their pigment content to maintain physiological balance [70]. The results of the present study indicated that the contents of Chl *a* and Car in *S. horneri* were significantly increased by warming under eutrophication. Similar results have been reported for other algae [71]. Therefore, the effective photosynthetic efficiency and maximum photosynthetic efficiency of PSII were clearly increased, and photosynthesis increased with increasing temperature. This is consistent with the research results of Zou and Gao [72] on *Gracilaria lemaneiformis*. Increased N concentration increases the pigment contents, key rate-limiting enzymes (i.e., Rubisco) and other N-containing compounds in the photosynthetic reaction; the substrate concentration in the photosynthetic process also increases, thus improving photosynthesis in algae [73,74]. However, under high N, warming counteracts this boost. A study of *Gracilaria lemaneiformis* showed that the photosynthetic rate of algae increased

with increasing temperature, but only if the temperature remains within an appropriate range [75]. The photosynthetic rate decreases at temperatures above or below the optimal temperature. When the optimal temperature of algae is exceeded, the higher the temperature, the lower the photosynthetic rate of algae. This suggests that high temperatures inhibit the activity of the Rubisco enzyme in photosynthesis and in response, the carboxylation ability of Rubisco decreases. It has been reported that in an environment with sufficient N availability when the absorption of N by algae exceeds the requirement for photosynthesis, the photosynthetic capacity of algae tends to be saturated by further increasing the N concentration [76]. It has also been shown that increasing N concentration may inhibit the photosynthesis of algae and decrease their photosynthetic capacity. This may be because the structure of photosynthetic proteins changed and photosystem II is inhibited at super-optimal temperatures [77,78]. It may also be that adapting to high temperatures may require higher investment in repair mechanisms, such as heat shock proteins, which may increase the need for N and other nutrients [79].

## 5. Conclusions

In summary, the reported results provide evidence that temperature rise and nitrogen enrichment could significantly affect the growth, photosynthetic performance, and biochemical composition of *S. horneri*. In particular, compared with the ambient temperature condition, increased temperature exerted an inhibitory effect on growth and photosynthesis, and this inhibitory effect was more significant under the nitrogen enrichment treatment. Accordingly, under the ongoing global warming coupled with eutrophication, the frequency and scale of gold tides caused by *S. horneri* would be reduced in the future.

**Author Contributions:** Conceptualization, H.W., X.L. and J.X.; Data curation, H.W. and X.L.; Formal analysis, J.X.; Funding acquisition, J.X.; Investigation, H.W., X.L., Y.L., C.W., C.J. and J.X.; Methodology, J.X.; Visualization, Y.L.; Writing—original draft, H.W., X.L. and Y.L.; Writing—review and editing, C.W., C.J. and J.X. All authors have read and agreed to the published version of the manuscript.

**Funding:** This study was supported by the Natural Science Foundation of Jiangsu Province (grant number BK20221398), National Natural Science Foundation of China (grant number 41706141), the Six Talents Peaks in Jiangsu Province (grant number JNHB-213), China Postdoctoral Science Foundation funded project (grant number 2018M632668), “333” project of Jiangsu Province, the Jiangsu Planned Projects for Postdoctoral Research Funds (grant number 2018K025A), “Haiyan project” of Lianyungang city (grant number 2018-ZD-005), “521 project” of Lianyungang city (grant number LYG06521202169), Open project of Jiangsu Institute of Marine Resources Development (grant number JSIMR202010), “Huaguoshan project” of Lianyungang City, the Lianyungang Planned Projects for Postdoctoral Research Funds.

**Institutional Review Board Statement:** Not applicable.

**Informed Consent Statement:** Not applicable.

**Data Availability Statement:** Data available on request due to restrictions, e.g., privacy or ethical. The data presented in this study are partially available on request from the corresponding author.

**Conflicts of Interest:** The authors declare no conflict of interest.

## References

1. Fontela, M.; Velo, A.; Gilcoto, M.; Pérez, F. Anthropogenic CO<sub>2</sub> and ocean acidification in Argentine Basin Water Masses over almost five decades of observations. *Sci. Total Environ.* **2021**, *779*, 146570. [[CrossRef](#)] [[PubMed](#)]
2. Scheffer, M.; Schulz, K.G.; Bellerby, R.G.J.; Botros, M.; Fritsche, P.; Meyerhöfer, M.; Neill, C.; Nondal, G.; Oschlies, A.; Wohlers, J.; et al. Positive feedback between global warming and atmospheric CO<sub>2</sub> concentration inferred from past climate change. *Geophys. Res. Lett.* **2006**, *33*, 229–237. [[CrossRef](#)]
3. Riebesell, U.; Schulz, K.G.; Bellerby, R.G.J.; Botros, M.; Fritsche, P.; Meyerhoefer, M.; Neill, C.; Nondal, G.; Oschlies, A.; Wohlers, J. Enhanced biological carbon consumption in a high CO<sub>2</sub> ocean. *Nature* **2007**, *450*, 545–548. [[CrossRef](#)] [[PubMed](#)]
4. Feely, R.A.; Doney, S.C.; Cooley, S.R. Ocean acidification: Present conditions and future changes in a high-CO<sub>2</sub> world. *Oceanography* **2009**, *22*, 36–47. [[CrossRef](#)]

5. Gattuso, J.P.; Magnan, A.; Billé, R.; Cheung, W.W.; Howes, E.L.; Joos, F.; Allemand, D.; Bopp, L.; Cooley, S.R.; Eakin, C.M.; et al. Contrasting futures for ocean and society from different anthropogenic CO<sub>2</sub> emissions scenarios. *Science* **2015**, *349*, aac4722. [[CrossRef](#)] [[PubMed](#)]
6. Collins, M.; Knutti, R.; Arblaster, J.; Dufresne, J.L.; Fichet, T.; Friedlingstein, P.; Gao, X.; Gutowski, W.J. Long-term climate change: Projections, commitments and irreversibility. Chapter 13; In *Climate Change 2013: The Physical Science Basis*; Cambridge University Press: London, UK, 2013; pp. 1029–1136. Available online: <https://www.issuelab.org/resource/climate-change-2013-the-physical-science-basis.html> (accessed on 15 June 2022).
7. Wernberg, T.; Russell, B.D.; Moore, P.J.; Ling, S.D.; Smale, D.A.; Campbell, A.C.; Melinda, A.; Steinberg, P.D.; Kendrick, G.A.; Connell, S.D. Impacts of climate change in a global hotspot for temperate marine biodiversity and ocean warming. *J. Exp. Mar. Biol. Ecol.* **2011**, *400*, 7–16. [[CrossRef](#)]
8. Kelaher, B.P.; Mamo, L.T.; Provost, E.; Litchfield, S.G.; Giles, A.; Butcherine, P. Influence of ocean warming and acidification on habitat-forming coralline algae and their associated molluscan assemblages. *Glob. Ecol. Conserv.* **2022**, *35*, e02081. [[CrossRef](#)]
9. Barbier, E.B.; Hacker, S.D.; Kennedy, C.; Koch, E.W.; Stier, A.C.; Silliman, B.R. The value of estuarine and coastal ecosystem services. *Ecol. Monogr.* **2011**, *81*, 169–193. [[CrossRef](#)]
10. Chung, I.K.; Beardall, J.; Mehta, S.; Sahoo, D.; Stojkovic, S. Using marine macroalgae for carbon sequestration: A critical appraisal. *J. Appl. Phycol.* **2010**, *23*, 877–886. [[CrossRef](#)]
11. Arina, N.; Raynusha, C.; Hidayah, N.; Zainee, N.F.A.; Prathep, A.; Rozaimi, M. Coralline macroalgae contribution to ecological services of carbon storage in a disturbed seagrass meadow. *Mar. Environ. Res.* **2020**, *162*, 105156. [[CrossRef](#)]
12. Krause-Jensen, D.; Duarte, C.M. Substantial role of macroalgae in marine carbon sequestration. *Nat. Geosci.* **2016**, *9*, 737–742. [[CrossRef](#)]
13. Sondak, C.F.A.; Ang, P.O.; Beardall, J.; Bellgrove, A.; Boo, S.M.; Gerung, G.S.; Hepburn, C.D.; Hong, D.D.; Hu, Z.Y.; Kawai, H.; et al. Carbon dioxide mitigation potential of seaweed aquaculture beds (SABs). *J. Appl. Phycol.* **2016**, *29*, 2363–2373. [[CrossRef](#)]
14. Yong, W.T.L.; Thien, V.Y.; Rupert, R.; Rodrigues, K.F. Seaweed: A potential climate change solution. *Renew. Sust. Energ. Rev.* **2022**, *159*, 112222. [[CrossRef](#)]
15. Wu, H.L.; Chen, J.; Feng, J.C.; Liu, Y.H.; Li, X.B.; Chen, R.; Xu, J.T. Thermal fluctuations and nitrogen enrichment synergistically accelerate biomass yield of *Pyropia haitanensis*. *Aquat. Bot.* **2022**, *179*, 103501. [[CrossRef](#)]
16. Wu, H.L.; Liu, Y.M.; Beardall, J.; Zhong, Z.H.; Gao, G.; Xu, J.T. Physiological acclimation of *Ulva prolifera* to seasonal environmental factors drives green tides in the Yellow Sea. *Mar. Environ. Res.* **2022**, *179*, 105695. [[CrossRef](#)]
17. Boyce, D.G.; Lewis, M.R.; Worm, B. Global phytoplankton decline over the past century. *Nature* **2010**, *466*, 591–596. [[CrossRef](#)]
18. Thomas, M.K.; Kremer, C.T.; Klausmeier, C.A.; Litchman, E. A global pattern of thermal adaptation in marine phytoplankton. *Science* **2012**, *338*, 1085–1088. [[CrossRef](#)]
19. Bopp, L.; Monfray, P.; Aumont, O.; Belviso, S. Potential impact of climate change on marine export production. *Global Biogeochem. Cycles* **2001**, *15*, 81–99. [[CrossRef](#)]
20. Steinacher, M.; Joos, F.; Frölicher, T.L.; Bopp, L. Projected 21st century decrease in marine productivity: A multi-model analysis. *Biogeosciences* **2009**, *7*, 979–1005. [[CrossRef](#)]
21. Figueroa, F.L.; Barufi, J.B.; Malta, E.J.; Condeálvarez, R.; Nitschke, U.; Arenas, F.; Mata, M.; Connan, S.; Abreu, M.H.; Marquardt, R. Short-term effects of increasing CO<sub>2</sub>, nitrate and temperature on three Mediterranean macroalgae: Biochemical composition. *Aquat. Biol.* **2014**, *22*, 177–193. [[CrossRef](#)]
22. Sobrino, C.; Neale, P.J. Short-term and long-term effects of temperature on photosynthesis in the diatom *Thalassiosira pseudonana* under UVR exposures. *J. Phycol.* **2007**, *43*, 426–436. [[CrossRef](#)]
23. Thomas, M.K.; Aranguren-Gassis, M.; Kremer, C.T.; Gould, M.R.; Anderson, K.; Klausmeier, C.A.; Litchman, E. Temperature-nutrient interactions exacerbate sensitivity to warming in phytoplankton. *Global Change Biol.* **2017**, *23*, 3269–3280. [[CrossRef](#)] [[PubMed](#)]
24. Schmid, M.; Guihéneuf, F.; Nitschke, U.; Stengel, D.B. Acclimation potential and biochemical response of four temperate macroalgae to light and future seasonal temperature scenario. *Algal Res.* **2021**, *54*, 102190. [[CrossRef](#)]
25. Litchman, E.; Pinto, P.D.T.; Klausmeier, C.A.; Thomas, M.K.; Yoshiyama, K. Linking traits to species diversity and community structure in phytoplankton. *Hydrobiologia* **2010**, *653*, 15–28. [[CrossRef](#)]
26. Xiong, Y.L.; Gao, L.; Qu, L.Y.; Xu, J.T.; Ma, Z.L.; Gao, G. The contribution of fish and seaweed mariculture to the coastal fluxes of biogenic elements in two important aquaculture areas, China. *Sci. Total Environ.* **2023**, *856*, 159056. [[CrossRef](#)] [[PubMed](#)]
27. Rabalais, N.N.; Turner, R.E.; Díaz, R.J.; Justić, D. Global change and eutrophication of coastal waters. *ICES J. Mar. Sci.* **2009**, *66*, 1528–1537. [[CrossRef](#)]
28. Shahar, B.; Guttman, L. Integrated biofilters with *Ulva* and periphyton to improve nitrogen removal from mariculture effluent. *Aquaculture* **2021**, *532*, 736011. [[CrossRef](#)]
29. Zhang, C.; Lu, J.; Wu, J. Enhanced removal of phenolic endocrine disrupting chemicals from coastal waters by intertidal macroalgae. *J. Hazard. Mater.* **2021**, *411*, 125105. [[CrossRef](#)]
30. Li, P.P.; Chen, H.H.; Zhang, J.Y.; Feng, X.Q.; Xiao, B.H.; Hu, Y.Y.; Sui, Z.H. Effects of nutrient deficiency on the branch phenotype of the macroalgae *Gracilariopsis lemaneiformis* (Rhodophyta). *Aquaculture* **2023**, *562*, 738794. [[CrossRef](#)]

31. Zhou, W.; Wu, H.; Huang, J.J.; Wang, J.G.; Zhen, W.; Wang, J.W.; Ni, J.X.; Xu, J.T. Elevated-CO<sub>2</sub> and nutrient limitation synergistically reduce the growth and photosynthetic performances of a commercial macroalga *Gracilariopsis lemaneiformis*. *Aquaculture* **2022**, *550*, 737878. [[CrossRef](#)]
32. Luo, M.B.; Liu, F.; Xu, Z.L. Growth and nutrient uptake capacity of two co-occurring species, *Ulva prolifera* and *Ulva linza*. *Aquat. Bot.* **2012**, *100*, 18–24. [[CrossRef](#)]
33. Fan, X.; Xu, D.; Wang, Y.T.; Zhang, X.W.; Cao, S.N.; Mou, S.L.; Ye, N.H. The effect of nutrient concentrations, nutrient ratios and temperature on photosynthesis and nutrient uptake by *Ulva prolifera*: Implications for the explosion in green tides. *J. Appl. Phycol.* **2013**, *26*, 537–544. [[CrossRef](#)]
34. Li, H.M.; Zhang, Y.Y.; Han, X.R.; Shi, X.Y.; Rivkin, R.B.; Legendre, L. Growth responses of *Ulva prolifera* to inorganic and organic nutrients: Implications for macroalgal blooms in the southern Yellow Sea, China. *Sci. Rep.* **2016**, *6*, 26498. [[CrossRef](#)] [[PubMed](#)]
35. Smetacek, V.; Zingone, A. Green and golden seaweed tides on the rise. *Nature* **2013**, *504*, 84–88. [[CrossRef](#)] [[PubMed](#)]
36. Zhuang, M.M.; Liu, J.L.; Ding, X.W.; He, J.Z.; Zhao, S.; Wu, L.J.; Gao, S.; Zhao, C.Y.; Liu, D.Y.; Zhang, J.H.; et al. Sargassum blooms in the East China Sea and Yellow Sea: Formation and management. *Mar. Pollut. Bull.* **2021**, *162*, 111845. [[CrossRef](#)] [[PubMed](#)]
37. Pang, S.J.; Liu, F.; Shan, T.F.; Gao, S.Q.; Zhang, Z.H. Cultivation of the brown alga *Sargassum horneri*: Sexual reproduction and seedling production in tank culture under reduced solar irradiance in ambient temperature. *J. Appl. Phycol.* **2009**, *21*, 413–422. [[CrossRef](#)]
38. Yoon, J.T.; Sun, S.M.; Chung, G. *Sargassum* bed restoration by transplantation of germlings grown under protective mesh cage. *J. Appl. Phycol.* **2014**, *26*, 505–509. [[CrossRef](#)]
39. Su, L.; Shan, T.F.; Pang, S.J.; Li, J. Analyses of the genetic structure of *Sargassum horneri* in the Yellow Sea: Implications of the temporal and spatial relations among floating and benthic populations. *J. Appl. Phycol.* **2018**, *30*, 1417–1424. [[CrossRef](#)]
40. Lapointe, B.E. A comparison of nutrient-limited productivity in *Sargassum natans* from neritic vs. oceanic waters of the western North Atlantic Ocean. *Limnol. Oceanogr.* **1995**, *40*, 625–633. [[CrossRef](#)]
41. Ohtake, M.; Natori, N.; Sugai, Y.; Tsuchiya, K.; Aketo, T.; Nishihara, G.N.; Toda, T. Growth and nutrient uptake characteristics of *Sargassum macrocarpum* cultivated with phosphorus-replete wastewater. *Aquat. Bot.* **2020**, *163*, 103208. [[CrossRef](#)]
42. Bao, M.L.; Park, J.S.; Wu, H.L.; Lee, H.J.; Park, S.R.; Kim, T.H.; Son, Y.B.; Lee, T.H.; Yarish, C.; Kim, J.K. A comparison of physiological responses between attached and pelagic populations of *Sargassum horneri* under nutrient and light limitation. *Mar. Environ. Res.* **2022**, *173*, 105544. [[CrossRef](#)] [[PubMed](#)]
43. Falkowski, P.G.; Barber, R.T.; Smetacek, V. Biogeochemical controls and feedbacks on ocean primary production. *Science* **1998**, *281*, 200–206. [[CrossRef](#)]
44. Elser, J.J.; Bracken, M.E.S.; Cleland, E.E.; Gruner, D.S.; Harpole, W.S.; Hillebrand, H.; Ngai, J.T.; Seabloom, E.W.; Shurin, J.B.; Smith, J.E. Global analysis of nitrogen and phosphorus limitation of primary producers in freshwater, marine and terrestrial ecosystems. *Ecol. Lett.* **2007**, *10*, 1135–1142. [[CrossRef](#)] [[PubMed](#)]
45. Hee, Y.Y.; Suratman, S.; Weston, K. Nutrient cycling and primary production in Peninsular Malaysia waters; regional variation and its causes in the South China Sea. *Estuar. Coast. Shelf Sci.* **2020**, *245*, 106947. [[CrossRef](#)]
46. Boyd, P.W.; Rynearson, T.A.; Armstrong, E.A.; Fu, F.X.; Hayashi, K.; Hu, Z.X.; Hutchins, D.A.; Kudela, R.M.; Litchman, E.; Mulholland, M.R.; et al. Marine phytoplankton temperature versus growth responses from polar to tropical waters—Outcome of a scientific community-wide study. *PLoS ONE* **2013**, *8*, e63091. [[CrossRef](#)] [[PubMed](#)]
47. Thomas, M.K.; Kremer, C.T.; Litchman, E. Environment and evolutionary history determine the global biogeography of phytoplankton temperature traits. *Global Ecol. Biogeogr.* **2016**, *25*, 75–86. [[CrossRef](#)]
48. IPCC. *Climate Change, 2014: Synthesis Report. Contribution of Working Groups I, II and III to the Fifth Assessment Report of the Intergovernmental Panel on Climate Change*; IPCC: Geneva, Switzerland, 2014; p. 151.
49. Genty, B.; Briantais, J.M.; Baker, N.R. The relationship between the quantum yield of photosynthetic electron transport and quenching of chlorophyll fluorescence. *Biochim. Biophys. Acta Gen. Subj.* **1989**, *990*, 87–92. [[CrossRef](#)]
50. Jassby, A.D.; Platt, T. Mathematical formulation of the relationship between photosynthesis and light for phytoplankton. *Limnol. Oceanogr.* **1976**, *21*, 540–547. [[CrossRef](#)]
51. Xu, Z.G.; Gao, G.; Xu, J.T.; Wu, H.L. Physiological response of a golden tide alga (*Sargassum muticum*) to the interaction of ocean acidification and phosphorus enrichment. *Biogeosciences* **2017**, *14*, 671–681. [[CrossRef](#)]
52. Wellburn, A.R. The spectral determination of chlorophylls a and b, as well as total carotenoids, using various solvents with spectrophotometers of different resolution. *J. Plant Physiol.* **1994**, *144*, 307–313. [[CrossRef](#)]
53. Kochert, G. *Protein Determination by Dye Binding*; Cambridge University Press: London, UK, 1978; pp. 91–93. [[CrossRef](#)]
54. Nishihara, G.N.; Noro, T.; Terada, R. Effect of temperature and light on the photosynthetic performance of two edible seaweeds: *Meristotheca coacta* Okamura and *Meristotheca papulosa* J. Agardh (Solieriaceae, Rhodophyta). *Aquac. Sci.* **2012**, *60*, 377–388. [[CrossRef](#)]
55. Kim, J.K.; Yarish, C.; Pereira, R. Tolerances to hypo-osmotic and temperature stresses in native and invasive species of *Gracilaria* (Rhodophyta). *Phycologia* **2019**, *55*, 257–264. [[CrossRef](#)]
56. Cui, J.J.; Zhang, J.H.; Huo, Y.Z.; Zhou, L.J.; Wu, Q.; Chen, L.P.; Yu, K.F.; He, P.M. Adaptability of free-floating green tide algae in the Yellow Sea to variable temperature and light intensity. *Mar. Pollut. Bull.* **2015**, *101*, 660–666. [[CrossRef](#)]
57. Wu, H.L.; Zhang, J.H.; Yarish, C.; He, P.M.; Kim, J.K. Bioremediation and nutrient migration during blooms of *Ulva* in the Yellow Sea, China. *Phycologia* **2018**, *57*, 223–231. [[CrossRef](#)]

58. Zhou, Z.X.; Yu, R.C.; Zhou, M.J. Evolution of harmful algal blooms in the East China Sea under eutrophication and warming scenarios. *Water Res.* **2022**, *221*, 118807. [CrossRef]
59. Wang, Y.; Zhong, Z.H.; Qin, S.; Li, J.L.; Liu, Z.Y. Effects of temperature and light on growth rate and photosynthetic characteristics of *Sargassum horneri*. *J. Ocean Univ. China* **2021**, *20*, 101–110. [CrossRef]
60. Zhang, P.; Wang, T.; Xie, Q.; Zhang, H.; Yan, X.; Chen, M. Effects of environment factors on growth of *Sargassum horneri* seedlings under indoor conditions. *J. Shanghai Ocean Univ.* **2014**, *23*, 200–207. Available online: [https://www.shhydx.com/shhy/ch/reader/create\\_pdf.aspx?file\\_no=20130800833&year\\_id=2014&quarter\\_id=2&falq=1](https://www.shhydx.com/shhy/ch/reader/create_pdf.aspx?file_no=20130800833&year_id=2014&quarter_id=2&falq=1) (accessed on 21 September 2022).
61. Wu, H.L.; Feng, J.C.; Li, X.S.; Zhao, C.Y.; Liu, Y.H.; Xu, J.T. Effects of increased CO<sub>2</sub> and temperature on the physiological characteristics of the golden tide blooming macroalgae *Sargassum horneri* in the Yellow Sea, China. *Mar. Pollut. Bull.* **2019**, *146*, 639–644. [CrossRef] [PubMed]
62. Padfield, D.; Lowe, C.; Buckling, A.; Ffrench-Constant, R.; Jennings, S.; Shelley, F.; Ólafsson, J.S.; Yvon-Durocher, G. Metabolic compensation constrains the temperature dependence of gross primary production. *Ecol. Lett.* **2017**, *20*, 1250–1260. [CrossRef] [PubMed]
63. Marañón, E.; Lorenzo, M.P.; Cermeño, P.; Mouriño-Carballido, B. Nutrient limitation suppresses the temperature dependence of phytoplankton metabolic rates. *ISME J.* **2018**, *12*, 1836. [CrossRef]
64. Deutsch, C.A.; Tewksbury, J.J.; Huey, R.B.; Sheldon, K.S.; Ghalambor, C.K.; Haak, D.C.; Martin, P.R. Impacts of climate warming on terrestrial ectotherms across latitude. *Proc. Natl. Acad. Sci. USA* **2008**, *105*, 6668–6672. [CrossRef] [PubMed]
65. Martin, T.L.; Huey, R.B. Why “suboptimal” is optimal: Jensen’s inequality and ectotherm thermal preferences. *Am. Nat.* **2008**, *171*, E102–E118. [CrossRef]
66. Mandal, S.; Islam, M.S.; Biswas, M.H.; Akter, S. A mathematical model applied to investigate the potential impact of global warming on marine ecosystems. *Appl. Math. Model.* **2022**, *101*, 19–37. [CrossRef]
67. Lobban, C.S.; Harrison, P.J.; Harrison, P.J. *Seaweed Ecology and Physiology*; Cambridge University Press: London, UK, 1994; p. 366. [CrossRef]
68. Bews, E.; Booher, L.; Polizzi, T.; Long, C.; Kim, J.H.; Edwards, M.S. Effects of salinity and nutrients on metabolism and growth of *Ulva lactuca*: Implications for bioremediation of coastal watersheds. *Mar. Pollut. Bull.* **2021**, *166*, 112199. [CrossRef] [PubMed]
69. Lapointe, B.E. Phosphorus-limited photosynthesis and growth of *Sargassum natans* and *Sargassum fluitans* (Phaeophyceae) in the western North Atlantic. *Deep Sea Res. Part A Oceanogr. Res. Pap.* **1986**, *33*, 391–399. [CrossRef]
70. Leung, J.Y.S.; Russell, B.D.; Coleman, M.A.; Kelaher, B.K.; Connell, S.D. Long-term thermal acclimation drives adaptive physiological adjustments of a marine gastropod to reduce sensitivity to climate change. *Sci. Total Environ.* **2021**, *771*, 145208. [CrossRef]
71. Zou, D.H.; Gao, K.S. The photosynthetic and respiratory responses to temperature and nitrogen supply in the marine green macroalga *Ulva conglobata* (Chlorophyta). *Phycologia* **2014**, *53*, 86–94. [CrossRef]
72. Zou, D.H.; Gao, K.S. Temperature response of photosynthetic light- and carbon-use characteristics in the red seaweed *Gracilaria lemaneiformis* (Gracilariiales, Rhodophyta). *J. Phycol.* **2014**, *50*, 366–375. [CrossRef]
73. Dawes, C.J.; Koch, E.W. Physiological responses of the red algae *Gracilaria verrucosa* and *G. tikvahiae* before and after nutrient enrichment. *Bull. Mar. Sci.* **1990**, *46*, 335–344. Available online: <https://www.ingentaconnect.com/content/umrsmas/bullmar/1990/00000046/00000002/art00007> (accessed on 10 August 2022).
74. Crawford, N.M. Nitrate: Nutrient and signal for plant growth. *Plant Cell* **1995**, *7*, 859–868. [CrossRef]
75. Liu, L.; Zou, D.H.; Jiang, H.; Chen, B.B.; Zeng, X.P. Effects of increased CO<sub>2</sub> and temperature on the growth and photosynthesis in the marine macroalga *Gracilaria lemaneiformis* from the coastal waters of South China. *J. Appl. Phycol.* **2017**, *30*, 1271–1280. [CrossRef]
76. Alcoverro, T.; Cerbián, E.; Ballesteros, E. The photosynthetic capacity of the seagrass *Posidonia oceanica*: Influence of nitrogen and light. *J. Appl. Phycol.* **2001**, *30*, 1271–1280. [CrossRef]
77. Fork, D.C.; Murata, N.; Sato, N. Effect of growth temperature on the lipid and fatty acid composition, and the dependence on temperature of light-induced redox reactions of cytochrome *f* and of light energy redistribution in the thermophilic blue-green alga *Synechococcus lividus*. *Plant Physiol.* **1979**, *63*, 524–530. [CrossRef] [PubMed]
78. Sendall, K.M.; Reich, P.B.; Zhao, C.; Hou, J.; Wei, X.; Stefanski, A.; Rice, K.; Rich, R.L.; Montgomery, R.A. Acclimation of photosynthetic temperature optima of temperate and boreal tree species in response to experimental forest warming. *Global Change Biol.* **2015**, *21*, 1342–1357. [CrossRef] [PubMed]
79. O’Donnell, D.R.; Hamman, C.R.; Johnson, E.C.; Kremer, C.T.; Klausmeier, C.A.; Litchman, E. Rapid thermal adaptation in a marine diatom reveals constraints and trade-offs. *Global Change Biol.* **2018**, *24*, 4554–4565. [CrossRef]